

Synthesis and Reactivity of Phosphametallacycles: Sterically Induced Epimerizations and Retrocycloadditions

Tricia L. Breen[†] and Douglas W. Stephan*

Department of Chemistry and Biochemistry, University of Windsor,
Windsor, Ontario, Canada N9B 3P4

Received August 16, 1996[⊗]

Elimination of methane from $\text{Cp}_2\text{Zr}(\text{PR}^*\text{H})(\text{Me})$ ($\text{R}^* = \text{C}_6\text{H}_2\text{-}2,4,6\text{-}t\text{-Bu}_3$) (**4**) in the presence of diphenylacetylene or phenylpropyne afforded the [2 + 2] cycloaddition products $\text{Cp}_2\text{Zr}(\text{P}(\text{R}^*)\text{C}(\text{Ph})=\text{CPh})$ (**3**) and $\text{Cp}_2\text{Zr}(\text{P}(\text{R}^*)\text{C}(\text{Me})=\text{CPh})$ (**5**), respectively. Alternatively, the [2 + 2] cycloaddition reaction between $(\text{Cp}_2\text{Zr}=\text{PR}^*)(\text{PMe}_3)$ (**1**) and phenylacetylene yielded $\text{Cp}_2\text{Zr}(\text{P}(\text{R}^*)\text{C}(\text{H})=\text{CPh})$ (**6**). Metallacycles **3** and **5** undergo facile [2 + 2] retrocycloaddition reactions; addition of 1 equiv of phenylpropyne to **3** resulted in an equilibrium mixture of **3** and **5**. In contrast, addition of phenylacetylene to **3** yielded $\text{Cp}_2\text{Zr}(\text{C}\equiv\text{CPh})(\text{C}(\text{Ph})=\text{C}(\text{Ph})\text{-P}(\text{R}^*))$ (**7**), the product of C–H activation of the terminal alkyne. Attempts to synthesize a phosphametallacycle with less sterically hindered substituents on phosphorus by reaction of Cp_2ZrMeCl , diphenylacetylene, and LiHPMe_3 ($\text{Me}_3 = \text{C}_6\text{H}_2\text{-}2,4,6\text{-Me}_3$) instead led to the formation of $\text{Cp}_2\text{Zr}(\text{P}(\text{Mes})\text{P}(\text{Mes})\text{C}(\text{Ph})=\text{CPh})$ (**8**). Probing the mechanism of formation of **8** by reaction of $(\text{Cp}_2\text{ZrCl})_2(\mu\text{-PMe}_3)$ with Li_2PMe_3 in the presence of diphenylacetylene afforded $\text{Cp}_2\text{Zr}(\text{P}(\text{Mes})\text{C}(\text{Ph})=\text{CPh})$ (**9**). However, reaction of **9** with H_2PMe_3 instead resulted in the formation of the unstable compound $\text{Cp}_2\text{Zr}(\text{C}(\text{Ph})=\text{C}(\text{Ph})\text{PMe}_3\text{H})(\text{PMe}_3\text{H})$ (**10**). Phosphametallacyclobutene **3** reacts with *tert*-butyl isocyanide, acetone, cyclohexanone, benzonitrile, benzaldehyde and styrene oxide to give the insertion products $\text{Cp}_2\text{Zr}(\text{C}(\text{N}=\text{t-Bu})\text{P}(\text{R}^*)\text{C}(\text{Ph})=\text{CPh})$ (**12**), $\text{Cp}_2\text{Zr}(\text{OCMe}_2\text{P}(\text{R}^*)\text{C}(\text{Ph})=\text{CPh})$ (**13**), $\text{Cp}_2\text{Zr}(\text{O}(\text{c-CC}_5\text{H}_{10})\text{P}(\text{R}^*)\text{C}(\text{Ph})=\text{CPh})$ (**14**), $\text{Cp}_2\text{Zr}(\text{N}=\text{C}(\text{Ph})\text{P}(\text{R}^*)\text{C}(\text{Ph})=\text{CPh})$ (**15**), $\text{Cp}_2\text{Zr}(\text{OCHPhP}(\text{R}^*)\text{C}(\text{Ph})=\text{CPh})$ (**16**), and $\text{Cp}_2\text{Zr}(\text{OCH}_2\text{CHPhP}(\text{R}^*)\text{C}(\text{Ph})=\text{CPh})$ (**17**), respectively. Compounds **16** and **17** were also obtained by reaction of either benzaldehyde or styrene oxide with **13**, **14**, or **15**, via [4 + 2] retrocycloadditions. Epimerization at phosphorus has been identified in complexes **3**, **5**, **6**, **8**, **9**, and **12–15**, and has been attributed to steric congestion in these species. Spectroscopic methods, X-ray crystallography, and molecular orbital calculations have been employed to address this issue.

Introduction

The [2 + 2] cycloaddition reaction with alkynes is one of the established reactivity patterns within the realm of metal-ligand multiple bonds.¹ This transformation has frequently occurred with Fischer carbenes;^{1,2} however, relatively few examples are known for Schrock alkylidenes^{1,3,4} and their multiply bonded heteroatomic

counterparts.^{5,6} Nonetheless, this reaction has been applied to group 4 metal alkylidenes, imides, oxides, and sulfides alike to yield metallacyclobutenes. Extensions of this approach to phosphorus chemistry have drawn less attention,⁷ although reports describing the preparation and structural studies of several terminal phosphinidenes ($\text{M}=\text{PR}$)^{8–10} and arsinidenes ($\text{M}=\text{AsR}$)¹¹ have appeared in the literature. In a preliminary communication¹² we have reported the first examples of phosphazirconacyclobutenes, obtained via [2 + 2] cycloaddition reactions of alkynes with either the terminal zirconium phosphinidene ($\text{Cp}_2\text{Zr}=\text{PR}^*)(\text{PMe}_3)$ (**1**; $\text{R}^* = 2,4,6\text{-}t\text{-Bu}_3\text{-C}_6\text{H}_2$) or the transient intermediate

* To whom correspondence should be addressed. E-mail: Stephan@UWindsor.ca.

[†] Current address: Department of Chemistry, Massachusetts Institute of Technology, Cambridge, MA 02139.

[⊗] Abstract published in *Advance ACS Abstracts*, December 1, 1996.

(1) Nugent, W. A.; Mayer, J. M. *Metal-Ligand Multiple Bonds*; Wiley: New York, 1988; and references cited therein.

(2) (a) Wulff, W. In *Advances in Metal-Organic Chemistry*; Liebeskind, L. S., Ed.; JAI: Greenwich, CT, 1989; Vol. 1. (b) Herndon, J. W.; Tumer, S. U.; McMullen, L. A.; Matasi, J. J.; Schnatter, W. F. K. In *Advances in Metal-Organic Chemistry; Volume 3* Liebeskind, L. S., Ed.; JAI: Greenwich, CT, 1994; Vol 3.

(3) (a) Tebbe, F. N.; Harlow, R. L. *J. Am. Chem. Soc.* **1980**, *102*, 6151. (b) McKinney, R. J.; Tulip, T. H.; Thorn, D. L.; Coolbaugh, T. S.; Tebbe, F. N. *J. Am. Chem. Soc.* **1981**, *103*, 5584.

(4) Wood, C. D.; McLain, S. J.; Schrock, R. R. *J. Am. Chem. Soc.* **1979**, *101*, 3210.

(5) (a) Carney, M. J.; Walsh, P. J.; Hollander, F. J.; Bergman, R. G. *J. Am. Chem. Soc.* **1989**, *111*, 8751. (b) Carney, M. J.; Walsh, P. J.; Bergman, R. G. *J. Am. Chem. Soc.* **1990**, *112*, 6426. (c) Carney, M. J.; Walsh, P. J.; Hollander, F. J.; Bergman, R. G. *Organometallics* **1992**, *11*, 761. (d) Polse, J. L.; Andersen, R. A.; Bergman, R. G. *J. Am. Chem. Soc.* **1995**, *117*, 5393.

(6) (a) Walsh, P. J.; Hollander, F. J.; Bergman, R. G. *J. Am. Chem. Soc.* **1988**, *110*, 8729. (b) Walsh, P. J.; Hollander, F. J.; Bergman, R. G. *Organometallics* **1993**, *12*, 3705. (c) Walsh, P. J.; Baranger, A. M.; Bergman, R. G. *J. Am. Chem. Soc.* **1992**, *114*, 1708. (d) Baranger, A. M.; Walsh, P. J.; Bergman, R. G. *J. Am. Chem. Soc.* **1993**, *115*, 2753.

[Cp₂Zr=PR*] (2). These metallacyclic products insert aldehyde, ketone, nitrile, epoxide, or isocyanate to afford five-, six-, and seven-membered phosphametallacycles, several of which undergo sterically induced [4 + 2] retrocycloadditions. Epimerization at phosphorus and the diastereoselectivity of the insertion reactions have been examined by employing spectroscopic methods and molecular orbital calculations. The ramifications of these results are considered herein.

Experimental Section

General Data. All preparations were performed under an atmosphere of dry, O₂-free N₂ either by Schlenk line techniques or with a Vacuum Atmospheres inert-atmosphere glovebox. Solvents were reagent grade, distilled from the appropriate drying agents under N₂, and degassed by the freeze-thaw method at least three times prior to use. All organic reagents were purified by conventional methods. ¹H and ¹³C{¹H} NMR spectra were recorded on a Bruker AC-300 operating at 300 and 75 MHz, respectively. ³¹P and ³¹P{¹H} NMR spectra were recorded on a Bruker AC-200 operating at 81 MHz. Trace amounts of protonated solvents were used as references, and chemical shifts are reported relative to SiMe₄ and 85% H₃PO₄, respectively. Low- and high-resolution EI mass spectral data were obtained employing a Kratos Profile mass spectrometer outfitted with a N₂ glovebag enclosure for the inlet port. Combustion analyses were performed by Galbraith Laboratories, Inc., Knoxville, TN, or Schwarzkopf Laboratories, Woodside, NY. H₂PR* and H₂PMes were purchased from the Quantum Design Chemical Co. All other reagents were purchased from the Aldrich Chemical Co. Cp₂ZrMeCl, ¹³(Cp₂Zr=PR*)(PMe₃) (1), ^{10c}Cp₂ZrMe(PHR*)(4), ^{10c}(Cp₂ZrCl)₂(*μ*-PMe₃), ¹⁴LiPHR*·3THF, ¹⁵LiPHMes·2THF, ¹⁶ and Li₂PMes¹⁷ were prepared by literature methods.

Synthesis of Cp₂Zr(P(R*)C(Ph)=CPh) (3) and Cp₂Zr(P(R*)C(Me)=CPh) (5). The preparations of 3 and 5 were performed in a similar manner; thus, only one procedure is described in detail. To a benzene solution of Cp₂ZrMeCl (272 mg, 1.0 mmol) and diphenylacetylene (178 mg, 1.0 mmol) was added a benzene solution of LiHPR*·3THF (501 mg, 1.0 mmol). The reaction mixture stood for 3 days, after which time the

dark red-brown solution was filtered and the solvent removed in vacuo. The oily residue was dissolved in diethyl ether, and the solvent was again evaporated under reduced pressure to yield a flaky red-gold solid. **3:** Yield: 588 mg (87%). ¹H NMR (25 °C, C₆D₆): δ 7.64 (d, |J| = 7.2 Hz, 2H, Ph H), 7.51 (d, [⁴J_{PH}] = 2.3 Hz, 2H, Ar H), 7.08–6.57 (m, 8H, Ph H), 5.74 (s, 10H, Cp), 1.54 (s, 18H, *o*-^tBu), 1.40 (s, 9H, *p*-^tBu). ¹³C{¹H} NMR (25 °C, C₆D₆): δ 210.6 (d, |J| = 15.1 Hz, quat), 152.3 (s, quat), 151.4 (d, |J| = 7.1 Hz, quat), 150.9 (s, quat), 149.2 (s, quat), 143.7 (s, quat), 141.1 (d, |J| = 43.8 Hz, quat), 131.0 (s, arom C–H), 128.1 (s, arom C–H), 127.4 (s, arom C–H), 125.6 (s, arom C–H), 125.5 (s, arom C–H), 123.8 (s, arom C–H), 120.9 (s, arom C–H), 112.4 (s, Cp), 38.0 (s, *o*-C(CH₃)₃), 34.7 (s, *p*-C(CH₃)₃), 33.4 (d, [⁴J_{PC}] = 7.9 Hz, *o*-C(CH₃)₃), 31.3 (s, *p*-C(CH₃)₃). ³¹P NMR (25 °C, C₆D₆): δ 55.3 (s). HRMS (EI): *m/e* calcd for C₄₂H₄₉PZr 674.2615, found 674.2605. **5:** Yield: 418 mg (68%). ¹H NMR (25 °C, C₆D₆) δ 7.52 (s, 2H, Ar H), 7.28–6.94 (m, 5H, Ph H), 5.73 (s, 10H, Cp), 2.17 (d, [³J_{PH}] = 5.6 Hz, 3H, CH₃), 1.67 (s, 18H, *o*-^tBu), 1.36 (s, 9H, *p*-^tBu). ¹³C{¹H} NMR (25 °C, C₆D₆): δ 207.0 (d, |J| = 14.5 Hz, quat), 152.5 (d, |J| = 6.8 Hz, quat), 148.9 (s, quat), 148.0 (s, quat), 145.3 (s, quat), 128.3 (s, arom C–H), 125.3 (s, arom C–H), 124.1 (s, arom C–H), 121.0 (s, arom C–H), 111.3 (s, Cp), 38.3 (s, *o*-C(CH₃)₃), 34.4 (s, *p*-C(CH₃)₃), 33.2 (d, [⁴J_{PC}] = 8.5 Hz, *o*-C(CH₃)₃), 31.3 (s, *p*-C(CH₃)₃), 22.4 (d, [²J_{PC}] = 16.9 Hz, CH₃). ³¹P NMR (25 °C, C₆D₆): δ 70.1 (s). HRMS (EI): *m/e* calcd for C₃₇H₄₇PZr 612.2458, found 612.2450.

Synthesis of Cp₂Zr(P(R*)C(H)=CPh) (6). To a benzene solution of 1 (115 mg, 0.2 mmol) was added a benzene solution of phenylacetylene (22.0 mL, 0.2 mmol). The reaction mixture stood for 3 h, after which time the dark brown solution was filtered and the solvent removed in vacuo. The oily residue was dissolved in pentane, and the volume was reduced under vacuum. Small red-brown crystals precipitated upon standing overnight and were isolated by filtration. Yield: 107 mg (89%). ¹H NMR (25 °C, C₆D₆): δ 7.61 (d, [²J_{PH}] = 5.4 Hz, 1H, =CH), 7.39 (d, [⁴J_{PH}] = 2.2 Hz, 2H, Ar H), 7.35–7.27 (m, 5H, Ph H), 5.60 (s, 10H, Cp), 1.71 (s, 18H, *o*-^tBu), 1.31 (s, 9H, *p*-^tBu). ¹³C{¹H} NMR (25 °C, C₆D₆): δ 215.0 (d, |J| = 11.6 Hz, quat), 150.9 (d, |J| = 6.2 Hz, quat), 147.6 (s, quat), 146.5 (s, quat), 144.2 (d, |J| = 20.0 Hz, quat), 128.6 (s, arom C–H), 127.9 (s, arom C–H), 127.2 (s, arom C–H), 120.8 (s, arom C–H), 110.0 (s, Cp), 104.5 (d, |J| = 74.5 Hz, P–CH), 38.1 (s, *o*-C(CH₃)₃), 34.2 (s, *p*-C(CH₃)₃), 33.1 (d, [⁴J_{PC}] = 8.5 Hz, *o*-C(CH₃)₃), 31.2 (s, *p*-C(CH₃)₃). ³¹P NMR (25 °C, C₆D₆): δ 85.0 (s).

Synthesis of Cp₂Zr(C≡CPh)(C(Ph)=C(Ph)PHR*) (7). To a benzene solution of 3 (135 mg, 0.2 mmol) was added phenylacetylene (22.0 mL, 0.2 mmol). The reaction mixture stood for 30 min, after which time the solvent was removed in vacuo and the product dissolved in hexane. When the solution stood for 12 h, a brown microcrystalline solid precipitated, which was isolated by filtration. Yield: 134 mg (86%). ¹H NMR (25 °C, C₆D₆): δ 7.50–7.43 (m, 3H, Ph H), 7.10–6.48 (m, 14H, Ph H), 6.78 (d, |J_{PH}| = 301.6 Hz, 1H, PH), 6.22 (s, 5H, Cp), 5.90 (s, 5H, Cp), 1.68 (s, 9H, *o*-^tBu), 1.62 (s, 9H, *o*-^tBu), 1.19 (s, 9H, *p*-^tBu). ¹³C{¹H} NMR (25 °C, C₆D₆): δ 203.4 (s, quat), 202.9 (s, quat), 157.9 (s, quat), 156.0 (d, |J| = 9.4 Hz, quat), 152.1 (s, quat), 151.5 (s, quat), 150.6 (s, quat), 149.8 (s, quat), 149.5 (s, quat), 138.7 (s, quat), 134.1 (d, |J| = 21.6 Hz, quat), 130.8 (d, |J| = 21.6 Hz, quat), 128.5 (s, arom C–H), 128.0 (s, arom C–H), 127.8 (s, arom C–H), 127.0 (s, arom C–H), 125.6 (s, arom C–H), 125.4 (s, arom C–H), 125.0 (s, arom C–H), 123.9 (s, arom C–H), 122.4 (br s, arom C–H), 122.3 (br s, arom C–H), 108.6 (s, Cp), 108.5 (s, Cp), 38.2 (s, *o*-C(CH₃)₃), 37.9 (s, *o*-C(CH₃)₃), 34.5 (s, *p*-C(CH₃)₃), 33.9 (s, *o*-C(CH₃)₃), 33.1 (d, |J| = 4.1 Hz, *o*-C(CH₃)₃), 31.2 (s, *p*-C(CH₃)₃). ³¹P NMR (25 °C, C₆D₆): δ -84.3 (d, |J_{PH}| = 300.9 Hz).

Synthesis of Cp₂Zr(P(Mes)P(Mes)C(Ph)=CPh) (8). To a benzene solution of Cp₂ZrMeCl (272 mg, 1.0 mmol) and diphenylacetylene (178 mg, 1.0 mmol) was added a benzene solution of LiHPMes·2THF (302 mg, 1.0 mmol). The reaction

(7) For examples of late-metal–phosphametallocyclobutenes see: (a) Al-Juaid, S. S.; Carmichael, D.; Hitchcock, P. B.; Lochschmidt, S.; Marinetti, A.; Mathey, F.; Nixon, J. F. *J. Chem. Soc., Chem. Commun.* **1988**, 1156. (b) Ajulu, F. A.; Carmichael, D.; Hitchcock, P. B.; Mathey, F.; Medidine, M. F.; Nixon, J. F.; Ricard, L.; Riley, M. L. *J. Chem. Soc., Chem. Commun.* **1992**, 750. (c) Ajulu, F. A.; Hitchcock, P. B.; Mathey, F.; Mechelin, R. A.; Nixon, J. F.; Pombeiro, A. J. L. *J. Chem. Soc., Chem. Commun.* **1993**, 142. (d) Al-Juaid, S. S.; Carmichael, D.; Hitchcock, P. B.; Marinetti, A.; Mathey, F.; Nixon, J. F. *J. Chem. Soc., Dalton Trans.* **1991**, 905. (e) Carmichael, D.; Hitchcock, P. B.; Nixon, J. F.; Mathey, F.; Ricard, L. *J. Chem. Soc., Dalton Trans.* **1993**, 1811. (f) Carmichael, D.; Hitchcock, P. B.; Nixon, J. F.; Mathey, F.; Ricard, L. *J. Chem. Soc., Chem. Commun.* **1989**, 1389.

(8) (a) Hitchcock, P. B.; Lappert, M. F.; Leung, W. P. *J. Chem. Soc., Chem. Commun.* **1987**, 1282. (b) Cowley, A. H.; Pellerin, B. *J. Am. Chem. Soc.* **1990**, 112, 6734.

(9) Cummins, C. C.; Schrock, R. R.; Davis, W. M. *Angew. Chem., Int. Ed. Engl.* **1993**, 32, 756.

(10) (a) Hou, Z.; Stephan, D. W. *J. Am. Chem. Soc.* **1992**, 114, 10088. (b) Hou, Z.; Breen, T. L.; Stephan, D. W. *Organometallics* **1993**, 12, 3158. (c) Breen, T. L.; Stephan, D. W. *J. Am. Chem. Soc.* **1995**, 117, 11914.

(11) Bonanno, J. B.; Wolczanski, P. T.; Lobkovsky, E. B. *J. Am. Chem. Soc.* **1994**, 116, 11159.

(12) Breen, T. L.; Stephan, D. W. *J. Am. Chem. Soc.* **1996**, 118, 4204.

(13) Jordan, R. F. *J. Organomet. Chem.* **1985**, 294, 321.

(14) Ho, J.; Stephan, D. W. *Organometallics*, **1991**, 10, 3001.

(15) Cowley, A. H.; Kilduff, J. E.; Newman, T. H.; Pakulski, M. J. *Am. Chem. Soc.* **1982**, 104, 5820.

(16) Hey, E.; Weller, F. *J. Chem. Soc., Chem. Commun.* **1988**, 782.

(17) (a) Hope, H.; Pestana, D. C.; Power, P. P. *Angew. Chem., Int. Ed. Engl.* **1991**, 30, 691. (b) Niediek, K.; Neumuller, B. *Z. Anorg. Allg. Chem.* **1993**, 619, 885.

mixture stood for 2 days, after which time the deep blue-green solution was filtered and the volume of the solution was reduced under vacuum. Hexamethyldisiloxane (ca. 6 mL) was added, and the solution was allowed to stand for 1 week. Dark wine red crystals were isolated by filtration and washed on the frit with hexane. Yield: 133 mg (19%). ^1H NMR (25 °C, C_6D_6): δ 7.47 (br d, $|J| = 1.8$ Hz, 2H, Ph *H*), 7.08–7.03 (m, 4H, Ph *H*), 6.92–6.86 (m, 3H, Ph *H*), 6.80–6.75 (m, 1H, Ph *H*), 6.62–6.58 (m, 4H, Ph *H*), 5.75 (v br s, 10H, Cp), 2.73 (s, 6H, *o*-Me), 2.68 (br s, 6H, *o*-Me), 2.22 (s, 3H, *p*-Me), 1.91 (s, 3H, *p*-Me). $^{13}\text{C}\{^1\text{H}\}$ NMR (25 °C, C_6D_6): δ 199.3 (dd, $|J| = 28.5$ Hz, $|J| = 4.1$ Hz, quat), 152.9 (d, $|J| = 7.3$ Hz, quat), 149.5 (s, quat), 143.5 (s, quat), 143.0 (s, quat), 141.8 (dd, $|J| = 13.3$ Hz, $|J| = 7.2$ Hz, quat), 141.5 (dd, $|J| = 42.8$ Hz, $|J| = 19.8$ Hz, quat), 138.6 (s, quat), 135.6 (s, quat), 133.8 (dd, $|J| = 26.3$ Hz, $|J| = 14.5$ Hz, quat), 130.8 (d, $|J| = 12.8$ Hz, arom *C*-H), 129.7 (br d, $|J| = 12.0$ Hz, arom *C*-H), 128.1 (s, arom *C*-H), 127.7 (s, arom *C*-H), 127.4 (s, arom *C*-H), 126.9 (br s, arom *C*-H), 126.2 (s, arom *C*-H), 123.2 (s, arom *C*-H), 110.5 (br s, Cp), 24.4 (d, $|J| = 9.7$ Hz, *o*-Me), 24.1 (d, $|J| = 9.5$ Hz, *o*-Me), 20.8 (s, *p*-Me), 20.5 (s, *p*-Me). ^{31}P NMR (25 °C, C_6D_6): δ 60.4 (d, $|J_{\text{PP}}| = 349.8$ Hz, Zr-*P*), -96.2 (d, $|J_{\text{PP}}| = 349.8$ Hz, P-*P*-C). ^1H NMR (-80 °C, $\text{CD}_3\text{C}_6\text{D}_5$): δ 7.20–6.49 (m, 14H, Mes *H* and Ph *H*), 5.88 (s, 5H, Cp), 5.29 (s, 5H, Cp), 2.86 (s, 3H, Me), 2.80 (s, 3H, Me), 2.58 (s, 3H, Me), 2.23 (s, 3H, Me), 2.11 (s, 3H, Me), 1.95 (s, 3H, Me). ^{31}P NMR (-80 °C, $\text{CD}_3\text{C}_6\text{D}_5$): δ 54.1 (d, $|J_{\text{PP}}| = 348.9$ Hz, Zr-*P*), -101.2 (d, $|J_{\text{PP}}| = 348.9$ Hz, P-*P*-C). Anal. Calcd for $\text{C}_{42}\text{H}_{42}\text{P}_2\text{Zr}$: C, 72.07; H, 6.05. Found: C, 72.33; H, 5.82.

Synthesis of $\text{Cp}_2\text{Zr}(\text{P}(\text{Mes})\text{C}(\text{Ph})=\text{CPh})$ (9). To a benzene suspension of $(\text{Cp}_2\text{ZrCl})_2(\mu\text{-PMes})$ (199 mg, 0.3 mmol) was added a benzene solution of diphenylacetylene (107 mg, 0.6 mmol) and a benzene suspension of Li_2PMes (54 mg, 0.33 mmol). The mixture was stirred vigorously for 2 days, after which time it was filtered. The solvent was removed in vacuo and the forest green product dissolved in diethyl ether. Reduction of the volume resulted in the precipitation of a deep green microcrystalline solid which was isolated by filtration. Yield: 267 mg (81%). ^1H NMR (25 °C, C_6D_6): δ 7.66 (d, $|J| = 8.0$ Hz, 2H, Ph *H*), 7.13–6.69 (m, 10H, Ph *H*), 5.83 (s, 10H, Cp), 2.28 (s, 6H, *o*-Me), 2.19 (s, 3H, *p*-Me). $^{13}\text{C}\{^1\text{H}\}$ NMR (25 °C, C_6D_6): δ 206.2 (d, $|J| = 17.0$ Hz, quat), 148.9 (d, $|J| = 4.9$ Hz, quat), 140.4 (d, $|J| = 12.1$ Hz, quat), 137.9 (d, $|J| = 12.2$ Hz, quat), 135.5 (s, quat), 131.4 (d, $|J| = 50.9$ Hz, quat), 131.3 (d, $|J| = 8.9$ Hz, arom *C*-H), 129.4 (s, arom *C*-H), 128.1 (s, arom *C*-H), 127.7 (s, arom *C*-H), 126.0 (s, arom *C*-H), 125.6 (s, arom *C*-H), 123.7 (s, arom *C*-H), 113.0 (s, Cp), 24.2 (s, Me), 23.9 (s, Me), 20.5 (s, Me). ^{31}P NMR (25 °C, C_6D_6): δ 31.4 (s).

Generation of $\text{Cp}_2\text{Zr}(\text{PHMes})(\text{C}(\text{Ph})\text{CPh}(\text{Mes}))$ (10). To a benzene suspension of **9** (20 mg, 0.05 mmol) was added a benzene solution of PH_2Mes (7 mg, 0.05 mmol). The mixture was stirred, and the reaction mixture was monitored by ^{31}P NMR spectroscopy. All attempts to isolate **10** were unsuccessful, as **10** proved to be unstable to air, moisture, and heat. ^{31}P NMR (25 °C, C_6D_6): δ -91.5 (m, Zr-*P*, $|J_{\text{PP}}| = 72$ Hz, $|J_{\text{PH}}| = 309.8$ Hz), -130.7 (dd, *C*-*P*, $|J_{\text{PP}}| = 72$ Hz, $|J_{\text{PH}}| = 205.4$ Hz).

Synthesis of $\text{Cp}_2\text{Zr}(\text{C}(\text{N-}t\text{Bu})\text{P}(\text{R}^*)\text{C}(\text{Ph})=\text{CPh})$ (12), $\text{Cp}_2\text{Zr}(\text{OCMe}_2\text{P}(\text{R}^*)\text{C}(\text{Ph})=\text{CPh})$ (13), $\text{Cp}_2\text{Zr}(\text{O}(\text{C-C}_6\text{H}_{11})\text{P}(\text{R}^*)\text{C}(\text{Ph})=\text{CPh})$ (14), $\text{Cp}_2\text{Zr}(\text{N}=\text{C}(\text{Ph})\text{P}(\text{R}^*)\text{C}(\text{Ph})=\text{CPh})$ (15), $\text{Cp}_2\text{Zr}(\text{OCHPhP}(\text{R}^*)\text{C}(\text{Ph})=\text{CPh})$ (16), and $\text{Cp}_2\text{Zr}(\text{OCH}_2\text{CHPhP}(\text{R}^*)\text{C}(\text{Ph})=\text{CPh})$ (17). The reactions of **3** with *tert*-butyl isocyanide, acetone, cyclohexanone, benzointrile, benzaldehyde, and styrene oxide were all performed in a similar manner; thus, only one preparation is described in detail. To a benzene solution of **3** (135 mg, 0.2 mmol) was added *tert*-butyl isocyanide (22.6 mL, 0.2 mmol). The reaction mixture stood for 30 min, after which time the solvent was removed in vacuo and the product dissolved in pentane. Large

yellow crystals formed over a 12 h period at room temperature and were isolated by filtration. **12**: yield 138 mg (91%). ^1H NMR (25 °C, C_6D_6): δ 7.52 (d, $|^4J_{\text{PH}}| = 2.1$ Hz, 2H, Ar *H*), 7.14–6.68 (m, 10H, Ph *H*), 5.65 (s, 10H, Cp), 1.64 (s, 18H, *o*-^{*t*}Bu), 1.23 (s, 9H, *p*-^{*t*}Bu), 1.08 (s, 9H, *p*-^{*t*}Bu). $^{13}\text{C}\{^1\text{H}\}$ NMR (25 °C, C_6D_6): δ 223.3 (d, $|J| = 43.6$ Hz, quat), 198.5 (d, $|J| = 38.9$ Hz, quat), 156.5 (s, quat), 156.3 (d, $|J| = 10.9$ Hz, quat), 153.2 (d, $|J| = 50.5$ Hz, quat), 151.2 (s, quat), 141.7 (d, $|J| = 32.0$ Hz, quat), 132.2 (d, $|J| = 55.6$ Hz, quat), 130.9 (s, arom *C*-H), 127.3 (s, arom *C*-H), 126.7 (s, arom *C*-H), 126.5 (s, arom *C*-H), 124.9 (s, arom *C*-H), 123.9 (d, $|J| = 7.1$ Hz, quat), 122.2 (s, arom *C*-H), 106.3 (s, Cp), 61.5 (s, N- $\text{C}(\text{CH}_3)_3$), 39.3 (s, *o*- $\text{C}(\text{CH}_3)_3$), 34.7 (s, *p*- $\text{C}(\text{CH}_3)_3$), 34.4 (d, $|^4J| = 4.5$ Hz, *o*- $\text{C}(\text{CH}_3)_3$), 31.0 (s, $\text{C}(\text{CH}_3)_3$), 29.8 (s, $\text{C}(\text{CH}_3)_3$). ^{31}P NMR (25 °C, C_6D_6): δ 17.8 (s). Anal. Calcd for $\text{C}_{47}\text{H}_{58}\text{NPZr}$: C, 74.36; H, 7.70. Found: C, 74.78; H, 7.47. **13**: yield 75 mg (51%). ^1H NMR (25 °C, C_6D_6): δ 7.38 (s, 2H, Ar *H*), 6.96–6.74 (m, 10H, Ph *H*), 5.94 (br s, 10H, Cp), 1.72 (br s, 18H, *o*-^{*t*}Bu), 1.54 (br s, 3H, Me), 1.50 (br s, 3H, Me), 1.23 (s, 9H, *p*-^{*t*}Bu). $^{13}\text{C}\{^1\text{H}\}$ NMR (25 °C, C_6D_6): δ 191.0 (d, $|J| = 31.5$ Hz, quat), 154.4 (br s, quat), 152.1 (d, $|J| = 7.0$ Hz, quat), 150.4 (s, quat), 149.7 (s, quat), 143.0 (d, $|J| = 19.8$ Hz, quat), 132.9 (d, $|J| = 65.4$ Hz, quat), 131.7 (s, arom *C*-H), 127.1 (s, arom *C*-H), 126.0 (s, arom *C*-H), 124.5 (s, arom *C*-H), 122.4 (br s, arom *C*-H), 121.4 (s, arom *C*-H), 110.8 (br s, Cp), 88.4 (d, $|J| = 36.0$ Hz, O-*C*), 39.8 (s, *o*- $\text{C}(\text{CH}_3)_3$), 39.7 (s, *o*- $\text{C}(\text{CH}_3)_3$), 35.2 (br s, *o*- $\text{C}(\text{CH}_3)_3$), 34.4 (s, *p*- $\text{C}(\text{CH}_3)_3$), 33.9 (s, Me), 33.8 (s, Me), 31.1 (s, *p*- $\text{C}(\text{CH}_3)_3$). ^{31}P NMR (25 °C, C_6D_6): δ 37.6 (s). ^1H NMR (-70 °C, $\text{CD}_3\text{C}_6\text{D}_5$, 200 MHz): δ 7.44 (br s, 2H, Ar *H*), 7.20–6.60 (m, 10H, Ph *H*), 6.10 (s, 5H, Cp), 5.79 (s, 5H, Cp), 1.86 (br s, 9H, *o*-^{*t*}Bu), 1.74–1.27 (br s, 24H, *o*-^{*t*}Bu, *p*-^{*t*}Bu, Me). ^{31}P NMR (-80 °C, $\text{CD}_3\text{C}_6\text{D}_5$): δ 36.1 (s). Anal. Calcd for $\text{C}_{45}\text{H}_{55}\text{OPZr}$: C, 73.62; H, 7.55. Found: C, 73.83; H, 7.68. **14**: yield 90 mg (58%). ^1H NMR (25 °C, C_6D_6): δ 7.52–6.70 (m, 12H, Ar *H* and Ph *H*), 6.11 (br s, 5H, Cp), 5.86 (br s, 5H, Cp), 2.35–1.20 (m, 10H, Cy *H*), 1.69 (br s, 18H, *o*-^{*t*}Bu), 1.23 (s, 9H, *p*-^{*t*}Bu). $^{13}\text{C}\{^1\text{H}\}$ NMR (25 °C, C_6D_6): δ 189.5 (d, $|J| = 29.0$ Hz, quat), 152.3 (d, $|J| = 8.3$ Hz, quat), 150.9 (s, quat), 150.3 (s, quat), 149.6 (s, quat), 143.5 (d, $|J| = 19.9$ Hz, quat), 132.0 (d, $|J| = 41.2$ Hz, quat), 132.8 (s, arom *C*-H), 126.8 (s, arom *C*-H), 126.5 (s, arom *C*-H), 125.2 (s, arom *C*-H), 122.7 (s, arom *C*-H), 111.4 (br s, Cp), 89.9 (d, $|J| = 31.2$ Hz, O-*C*), 40.2 (s, *o*- $\text{C}(\text{CH}_3)_3$), 35.5 (br s, *o*- $\text{C}(\text{CH}_3)_3$), 34.5 (s, *p*- $\text{C}(\text{CH}_3)_3$), 31.1 (s, *p*- $\text{C}(\text{CH}_3)_3$), 25.6 (s, CH_2), 22.7 (s, CH_2), 22.5 (d, $|J| = 8.4$ Hz, CH_2). ^{31}P NMR (25 °C, C_6D_6): δ 37.4 (s). ^1H NMR (-80 °C, $\text{CD}_3\text{C}_6\text{D}_5$, 200 MHz): δ 7.79–6.65 (m, 12H, Ar *H* and Ph *H*), 6.17 (s, 5H, Cp), 5.67 (s, 5H, Cp), 2.4–1.2 (v br, 28H, *o*-^{*t*}Bu, Cy *H*), 1.28 (s, 9H, *p*-^{*t*}Bu). ^{31}P NMR (-80 °C, $\text{CD}_3\text{C}_6\text{D}_5$): δ 31.6 (s). Anal. Calcd for $\text{C}_{48}\text{H}_{59}\text{OPZr}$: C, 74.47; H, 7.68. Found: C, 74.88; H, 7.41. **15**: yield 72 mg (46%). ^1H NMR (25 °C, C_6D_6): δ 7.60 (d, $|^4J_{\text{PH}}| = 2.2$ Hz, 2H, Ar *H*), 7.45–6.70 (m, 15H, Ph *H*), 5.89 (br s, 10H, Cp), 1.62 (br s, 18H, *o*-^{*t*}Bu), 1.24 (s, 9H, *p*-^{*t*}Bu). $^{13}\text{C}\{^1\text{H}\}$ NMR (25 °C, C_6D_6): δ 198.3 (d, $|J| = 31.2$ Hz, quat), 180.3 (d, $|J| = 36.4$ Hz, quat), 153.6 (d, $|J| = 13.3$ Hz, quat), 151.7 (s, quat), 145.8 (d, $|J| = 6.5$ Hz, quat), 142.7 (d, $|J| = 22.3$ Hz, quat), 138.0 (d, $|J| = 42.5$ Hz, quat), 131.7 (s, arom *C*-H), 129.4 (s, arom *C*-H), 128.6 (s, arom *C*-H), 126.9 (s, arom *C*-H), 126.5 (s, arom *C*-H), 125.2 (s, arom *C*-H), 122.3 (s, arom *C*-H), 109.0 (br s, Cp), 40.4 (br s, *o*- $\text{C}(\text{CH}_3)_3$), 34.8 (s, *p*- $\text{C}(\text{CH}_3)_3$), 34.4 (br s, *o*- $\text{C}(\text{CH}_3)_3$), 31.0 (s, *p*- $\text{C}(\text{CH}_3)_3$). ^{31}P NMR (25 °C, C_6D_6): δ 21.3 (s). ^1H NMR (-60 °C, $\text{CD}_3\text{C}_6\text{D}_5$, 200 MHz): δ 7.36–6.66 (m, 17H, Ar *H* and Ph *H*), 6.05 (s, 5H, Cp), 5.60 (s, 5H, Cp), 1.64 (br s, 9H, *o*-^{*t*}Bu), 1.57 (br s, 9H, *o*-^{*t*}Bu), 1.29 (s, 9H, *p*-^{*t*}Bu). ^{31}P NMR (-60 °C, $\text{CD}_3\text{C}_6\text{D}_5$): δ 21.5 (s). Anal. Calcd for $\text{C}_{49}\text{H}_{54}\text{NPZr}$: C, 75.53; H, 6.99. Found: C, 75.19; H, 6.75. **16**: yield 95 mg (61%). ^1H NMR (25 °C, C_6D_6): δ 7.81 (d, $|J| = 1.9$ Hz, 1H, *C*-H), 7.40–6.66 (m, 17H, Ph *H* and Ar *H*), 6.45 (s, 5H, Cp), 5.73 (s, 5H, Cp), 2.06 (s, 9H, ^{*t*}Bu), 1.28 (s, 9H, ^{*t*}Bu), 1.10 (s, 9H, ^{*t*}Bu). $^{13}\text{C}\{^1\text{H}\}$ NMR (25 °C, C_6D_6): δ 188.3 (d, $|J| = 33.9$ Hz, quat), 160.3 (s, quat), 159.9 (s, quat), 155.6 (d, $|J| = 5.3$ Hz, quat), 152.3 (d, $|J| = 9.6$ Hz, quat), 150.5 (d, $|J| = 48.2$ Hz, quat), 150.4 (s,

Table 1. Crystallographic Data

	8	12	13	14	16	17
formula	C ₄₂ H ₄₂ P ₂ Zr	C ₄₇ H ₅₈ NPZr	C ₄₅ H ₅₅ OPZr	C ₄₈ H ₅₉ OPZr	C ₄₉ H ₅₅ OPZr	C ₅₀ H ₅₇ OPZr
fw	699.96	759.18	734.12	774.19	782.17	796.19
cryst size (mm)	0.35 × 0.27 × 0.33	0.23 × 0.25 × 0.26	0.44 × 0.22 × 0.30	0.22 × 0.21 × 0.45	0.31 × 0.20 × 0.23	0.32 × 0.37 × 0.30
a, Å	16.61(1)	11.326(4)	13.26(1)	13.939(2)	31.385(6)	9.944(4)
b, Å	10.018(9)	21.129(6)	15.414(6)	15.083(2)	16.316(4)	41.12(2)
c, Å	21.215(5)	10.256(4)	11.085(8)	11.157(2)	16.685(4)	10.974(2)
α, deg		90.08(3)	101.75(5)	102.15(2)		
β, deg	93.60(4)	112.37(2)	112.10(5)	112.25(2)	95.86(2)	106.37(3)
γ, deg		93.70(3)	94.96(5)	94.43(1)		
V, Å ³	3522(3)	2263(1)	2021(2)	2073.0(9)	8620(2)	4305(2)
cryst syst	monoclinic	triclinic	triclinic	triclinic	monoclinic	monoclinic
space group	<i>P</i> 2 ₁ / <i>n</i>	<i>P</i> 1	<i>P</i> 1	<i>P</i> 1	<i>C</i> c	<i>P</i> 1
Z	4	4	2	2	8	4
μ, (cm ⁻¹)	4.31	3.10	3.42	3.38	3.26	3.27
d(calcd), g/cm ³	1.32	1.11	1.21	1.24	1.21	1.23
scan speed, deg/min	8	16	16	8	8	8
index range	<i>h, k, ±l</i>	<i>h, ±k, ±l</i>	<i>±h, ±k, l</i>	<i>h, ±k, ±l</i>	<i>±h, k, l</i>	<i>±h, k, l</i>
no. of data collected	6584	7977	7463.00	7299	4829	8171
no. of data <i>F</i> _o ² > 3σ(<i>F</i> _o ²)	1015	4051	2495	3268	1540	2707
no. of variables	196	451	208	370	248	229
transmissn factors	0.936–1.000	0.936–1.000	0.848–1.058	0.922–1.000	0.955–1.000	0.731–1.000
<i>R</i> , <i>R</i> _w , % ^a	6.45, 7.72	6.23, 6.32	8.0, 6.7	5.14, 6.35	7.8, 6.3	9.5, 7.6
goodness of fit	1.72	1.87	1.78	1.46	1.53	2.34

$$^a R = \sum(|F_o| - |F_c|)/\sum|F_o|; R_w = [\sum(|F_o| - |F_c|)^2/\sum|F_o|^2]^{0.5}.$$

quat), 144.4 (d, |*J*| = 24.3 Hz, quat), 143.5 (d, |*J*| = 14.8 Hz, quat), 132.9 (s, arom C–H), 131.4 (s, arom C–H), 126.3 (s, arom C–H), 125.6 (s, arom C–H), 125.2 (s, arom C–H), 123.0 (s, arom C–H), 122.8 (s, arom C–H), 112.7 (s, Cp), 112.1 (s, Cp), 89.0 (d, |*J*_{PC}| = 16.6 Hz, O–CH), 41.1 (s, *o*-C(CH₃)₃), 39.2 (d, |*J*_{PC}| = 6.9 Hz, *o*-C(CH₃)₃), 36.5 (s, *o*-C(CH₃)₃), 34.6 (s, *p*-C(CH₃)₃), 33.3 (d, |*J*_{PC}| = 18.1 Hz, *o*-C(CH₃)₃), 31.1 (s, *p*-C(CH₃)₃). ³¹P NMR (25 °C, C₆D₆): δ 13.9 (s). Anal. Calcd for C₄₉H₅₅OPZr: C, 75.24; H, 7.09. Found: C, 75.10; H, 7.14. **17**: yield 108 mg (68%). ¹H NMR (25 °C, C₆D₆): δ 7.56 (dd, |*J*| = 5.2 Hz, |*J*| = 1.9 Hz, 2H, Ar *H*), 7.11–6.53 (m, 15H, Ph *H*), 6.21 (s, 5H, Cp), 5.85 (s, 5H, Cp), 4.60 (m, 1H, C–H), 4.50 (m, 1H, C–H), 3.82 (m, 1H, C–H), 1.99 (s, 9H, *o*-*t*Bu), 1.32 (s, 9H, *o*-*t*Bu), 1.10 (s, 9H, *p*-*t*Bu). ¹³C{¹H} NMR (25 °C, C₆D₆): δ 192.6 (d, |*J*| = 53.3 Hz, quat), 157.4 (d, |*J*| = 35.3 Hz, quat), 156.6 (s, quat), 156.0 (d, |*J*| = 42.0 Hz, quat), 151.9 (d, |*J*| = 16.8 Hz, quat), 150.0 (s, quat), 144.5 (d, |*J*| = 7.8 Hz, quat), 141.4 (s, quat), 131.7 (s, arom C–H), 130.5 (s, arom C–H), 129.9 (d, |*J*| = 41.4 Hz, quat), 126.6 (s, arom C–H), 125.8 (s, arom C–H), 125.7 (s, arom C–H), 124.2 (s, arom C–H), 122.7 (d, |*J*| = 14.3 Hz, arom C–H), 122.4 (s, arom C–H), 112.1 (s, Cp), 112.0 (s, Cp), 80.9 (d, |*J*_{PC}| = 24.6 Hz, O–CH₂), 59.6 (d, |*J*_{PC}| = 41.1 Hz, CH), 40.4 (d, |*J*_{PC}| = 7.6 Hz, *o*-C(CH₃)₃), 40.0 (s, *o*-C(CH₃)₃), 34.8 (d, |*J*_{PC}| = 18.1 Hz, *o*-C(CH₃)₃), 34.6 (s, *p*-C(CH₃)₃), 34.4 (s, *o*-C(CH₃)₃), 31.1 (s, *p*-C(CH₃)₃). ³¹P NMR (25 °C, C₆D₆): δ -2.4 (d, |*J*| = 13.9 Hz). Anal. Calcd for C₅₀H₅₇OPZr: C, 75.43; H, 7.22. Found: C, 75.86; H, 7.16.

Kinetic Studies. NMR scale reactions were monitored as a function of time by ³¹P NMR spectroscopy. Integrations of the resonances were measured against an internal standard of PPh₃, which was shown separately to be inert.

X-ray Data Collection and Reduction. X-ray-quality crystals of **8**, **12**–**14**, **16**, and **17** were obtained directly from the preparation as described above. The crystals were manipulated and mounted in capillaries in a glovebox, thus maintaining a dry, O₂-free environment for each crystal. Diffraction experiments were performed at 24 °C on a Rigaku AFC5 diffractometer equipped with graphite-monochromatized Mo Kα (0.710 69 Å) radiation. The initial orientation matrix was obtained from 20 machine-centered reflections selected by an automated peak search routine. These data were used to determine the crystal systems. Automated Laue system check routines around each axis were consistent with the

crystal system. Ultimately, 25 reflections (20° < 2θ < 25°) were used to obtain the final lattice parameters and the orientation matrices. Crystal data are summarized in Table 1. The observed extinctions were consistent with the space groups. The data sets were collected in three shells (4.5° < 2θ < 50.0°), and 3 standard reflections were recorded every 197 reflections. Fixed scan rates were employed. Up to 4 repetitive scans of each reflection at the respective scan rates were averaged to ensure meaningful statistics. In all cases the background/scan time ratio was 0.5 and the scan range was from 1.0° below Kα₁ to 1.0° above Kα₂. The number of scans of each reflection was determined by the intensity. The intensities of the standards showed no statistically significant change over the duration of the data collections. The data were processed using the TEXSAN crystal solution package operating on a SGI Challenger mainframe with remote X-terminals. The reflections with *F*_o² > 3σ(*F*_o²) were used in the refinements.

Structure Solution and Refinement. Non-hydrogen atomic scattering factors were taken from the literature tabulations.^{18,19} The zirconium atom positions were determined using direct methods by employing either the SHELX-86 or direct-methods routines. The remaining non-hydrogen atoms were located from successive difference Fourier map calculations. The refinements were carried out by using full-matrix least-squares techniques on *F*, minimizing the function $w(|F_o| - |F_c|)^2$, where the weight *w* is defined as 4*F*_o²/2σ(*F*_o²) and *F*_o and *F*_c are the observed and calculated structure factor amplitudes. In the final cycles of each refinement, the number of non-hydrogen atoms that were assigned anisotropic temperature factors was limited so as to maintain a reasonable data to variable ratio. Empirical absorption corrections were applied to the data sets based on ψ-scan data. Hydrogen atom positions were calculated and allowed to ride on the carbon to which they are bonded, assuming a C–H bond length of 0.95 Å. Hydrogen atom temperature factors were fixed at 1.10 times the isotropic temperature factor of the carbon atom to which they are bonded. The hydrogen atom contributions were calculated but not refined. The final values of *R*, *R*_w, and the

(18) Cromer, D. T.; Mann, J. B. *Acta Crystallogr., Sect. A: Cryst. Phys. Theor. Gen. Crystallogr.* **1968**, A24, 324. (b) *Ibid.* **1968**, A24, 390.

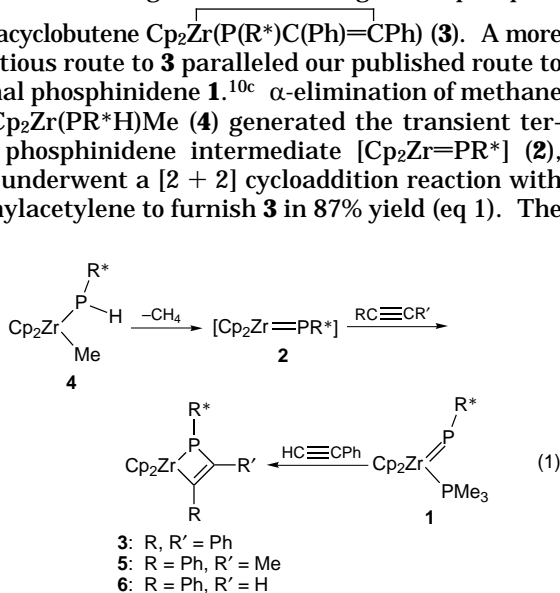
(19) Cromer, D. T.; Waber, J. T. *International Tables for X-ray Crystallography*; Kynoch Press: Birmingham, England, 1974.

maximum Δ/σ on any of the parameters in the final cycles of the refinements are given in Table 1. The locations of the largest peaks in the final difference Fourier map calculation as well as the magnitude of the residual electron densities in each case were of no chemical significance. The phenyl rings in **16** were refined with a constrained geometry in order to maintain a statistically meaningful data to variable ratio, and the correct enantiomorph was confirmed by inversion and refinement of the model. Positional parameters, hydrogen atom parameters, thermal parameters and bond distances and angles have been deposited as Supporting Information.

EHMO Calculations. Extended Huckel molecular orbital (EHMO) calculations were performed on a PowerMac 7100 workstation employing the CaChe software package.²⁰ Models were constructed on the basis of idealized geometries derived from related crystallographic data.

Results and Discussion

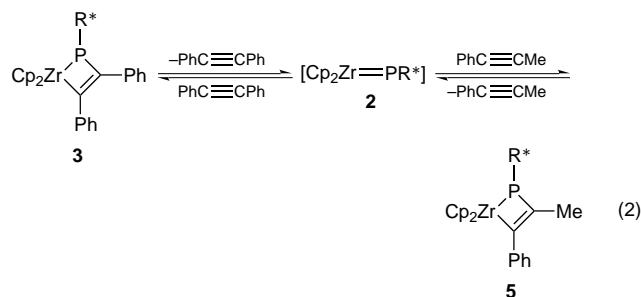
Synthesis of Phosphametallacycles. The reaction of terminal phosphinidene complex **1** with 1 equiv of diphenylacetylene proceeded slowly only when the released trimethylphosphine was successively removed from solution under vacuum, resulting in the observation of a singlet at 55.3 ppm in the ³¹P NMR spectrum of the reaction mixture. ¹H and ¹³C{¹H} NMR data supported the assignment of this signal as phosphametallacyclobutene $\text{Cp}_2\text{Zr}(\text{P}(\text{R}^*)\text{C}(\text{Ph})=\text{CPh})$ (**3**). A more expeditious route to **3** paralleled our published route to terminal phosphinidene **1**.^{10c} α -elimination of methane from $\text{Cp}_2\text{Zr}(\text{PR}^*\text{H})\text{Me}$ (**4**) generated the transient terminal phosphinidene intermediate $[\text{Cp}_2\text{Zr}=\text{PR}^*]$ (**2**), which underwent a [2 + 2] cycloaddition reaction with diphenylacetylene to furnish **3** in 87% yield (eq 1). The



use of 1-phenylpropyne as a trapping agent gave a 68% yield of $\text{Cp}_2\text{Zr}(\text{P}(\text{R}^*)\text{C}(\text{Me})=\text{CPh})$ (**5**); however, attempts to use phenylacetylene only resulted in the formation of product mixtures, presumably arising from C–H bond metathesis pathways. Nonetheless, reaction of **1** with phenylacetylene proceeded much more rapidly than with other alkynes to cleanly provide $\text{Cp}_2\text{Zr}(\text{P}(\text{R}^*)\text{C}(\text{H})=\text{CPh})$ (**6**) in 89% yield (eq 1). It is noteworthy that reactions involving unsymmetrical alkynes are completely regioselective, exclusively producing complexes in which the phenyl substituent is located α to the metal. These observations are consistent with the trend previously observed by Bergman *et al.* for zirconocene oxo, sulfido,^{5b–d} and imido complexes.⁶

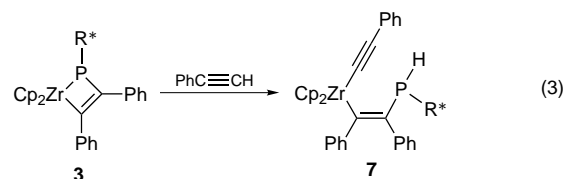
(20) CaChe Worksystem Software is an integrated modeling, molecular mechanics, and molecular orbital computational software package and is a product of CaChe Scientific Inc.

The reversible formation of metallacycles **3** and **5** was illustrated by the addition of trimethylphosphine to either complex, which rapidly resulted in the quantitative conversion to **1** along with the liberation of alkyne. Similarly, addition of 1 equiv of 1-phenylpropyne to **3** resulted in alkyne exchange to give an equilibrium mixture of **3** and **5** ($K_{\text{eq}} = 1.1$ at 25 °C) (eq 2).



Comparable to related oxo-,^{5b–d} thia-^{5b,c} and azametallacyclobutenes,⁶ these reactions are thought to occur through [2 + 2] retrocycloadditions to generate the transient intermediate $[\text{Cp}_2\text{Zr}=\text{PR}^*]$ (**2**), which then reacts with either PMe_3 or alkyne.

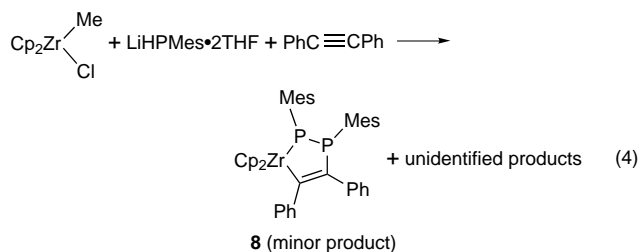
In contrast to the above results, **3** did not undergo exchange reactions with phenylacetylene; rather, C–H activation across the Zr–P bond of **3** resulted in the formation of the zirconocene alkynyl alkenyl complex $\text{Cp}_2\text{Zr}(\text{C}\equiv\text{CPh})(\text{CPh}=\text{C}(\text{Ph})\text{P}(\text{R}^*))$ (**7**), which was isolated in 86% yield (eq 3). The secondary phosphine



moiety in **7** was indicated by the ³¹P NMR signal at –84.9 ppm with a one-bond P–H coupling constant of 300.9 Hz. Furthermore, signals at 203.4 and 202.9 ppm in the ¹³C{¹H} NMR spectrum were indicative of two quaternary carbons bound to zirconium. Compound **7** is similar to $\text{Cp}_2\text{Zr}(\text{C}\equiv\text{CPh})(\text{C}(\text{Ph})=\text{C}(\text{H})\text{P}(\text{SiMe}_3)_2)$, which has recently been prepared by Hey-Hawkins *et al.* via insertion of phenylacetylene into the Zr–P bond of $\text{Cp}_2\text{Zr}(\text{P}(\text{SiMe}_3)_2)(\text{Cl})$, followed by reaction with lithium phenylacetylide.²¹ It is interesting that the Zr=P multiple bond of **1** tolerates the C–H group of the terminal alkyne, while the Zr–P single bond of metallacycle **3** does not. Presumably, the [2 + 2] retrocycloaddition of **3** that generates intermediate **2** is far slower than acidolysis of the Zr–P single bond of **3** by the acetylenic C–H group.

The analogue of **3** incorporating the less sterically hindered mesityl substituent on phosphorus was anticipated from the reaction of Cp_2ZrMeCl and $\text{LiHPMes}\cdot 2\text{THF}$ (Mes = $\text{C}_6\text{H}_2\text{-2,4,6-Me}_3$) in the presence of diphenylacetylene. However, fractional crystallization of the resulting complex mixture of products instead gave **8** (eq 4), which exhibited signals in the ³¹P NMR spectrum at 60.4 and –96.2 ppm with a P–P coupling constant of 349.8 Hz. ¹H and ¹³C{¹H} NMR data were consistent

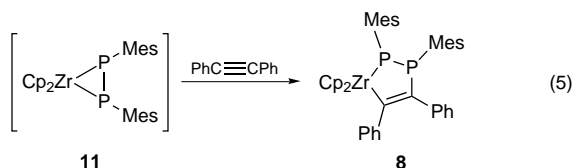
(21) (a) Hey-Hawkins, E.; Lindenberg, F. *Chem. Ber.* **1992**, *125*, 1815. (b) Lindenberg, F.; Hey-Hawkins, E. *Z. Anorg. Allg. Chem.* **1995**, *621*, 1531.



with the formulation of **8** as the diphosphametallacyclopentene $\text{Cp}_2\text{Zr}(\text{P}(\text{Mes})\text{P}(\text{Mes})\text{C}(\text{Ph})=\text{CPh})$, the structure of which was subsequently confirmed by an X-ray crystallographic study (Figure 1). The geometry about each phosphorus atom is pyramidal, and steric congestion in the metallacycle is minimized by the *transoid* disposition of the mesityl substituents. The Zr–P bond length of 2.596(9) Å compares well with the shorter Zr–P distance in the five-membered diphosphazirconacycle ($\eta^5\text{-C}_5\text{H}_3(\text{SiMe}_3)_2$) $_2\text{Zr}(\text{P}(\text{Ph})\text{C}_6\text{H}_4\text{PPh-1,2})$ (2.560(4) Å).²²

The mechanism of formation of **8** is not clear. One possibility is that the highly reactive terminal phosphinidene intermediate [$\text{Cp}_2\text{Zr}=\text{PMes}$] is generated and trapped by cycloaddition with diphenylacetylene to give the intermediate phosphametallacyclobutene $\text{Cp}_2\text{Zr}(\text{P}(\text{Mes})\text{C}(\text{Ph})=\text{CPh})$ **9**. Further reaction with 1 equiv of primary phosphine H_2PMes and elimination of hydrogen would then produce **8** (Scheme 1). In order to probe the mechanism, an alternative synthetic route to **9** was devised. Reaction of $(\text{Cp}_2\text{ZrCl})_2(\mu\text{-PMes})$ ¹⁴ with Li_2PMes in the presence of diphenylacetylene successfully yielded **9** in 81% yield. This species was analogous in ¹H and ¹³C{¹H} NMR spectra to metallacycles **3**, **5**, and **6**. However, subsequent reaction of **9** with 1 equiv of H_2PMes yielded the zirconocene alkenyl phosphide $\text{Cp}_2\text{Zr}(\text{C}(\text{Ph})=\text{C}(\text{Ph})\text{PMesH}(\text{PMesH}))$ (**10**), which proved to be very unstable and thus not isolable. The formation of **8** was not detected in solutions of **9** or **10** upon aging for several weeks or heating to 100 °C, thus dismissing both species as intermediates en route to **8**.

The most probable mechanism for the formation of **8** involves the generation of the unstable diphosphametallacyclopentane $\text{Cp}_2\text{Zr}(\text{P}_2\text{Mes}_2)$ (**11**), which is trapped through insertion of diphenylacetylene into a Zr–P bond (eq 5). Sterically demanding cyclopentadienyl ligands



have been reported to stabilize diphosphametallacyclopentanes,^{10b,23} and insertion of alkyne into the Zr–P bond of an acyclic phosphide has been previously observed by Hey-Hawkins *et al.*²¹ The proposed mechanism is also comparable to the insertion of alkyne into the Zr–N bond of the (η^2 -1,2-diphenylhydrazido)zir-

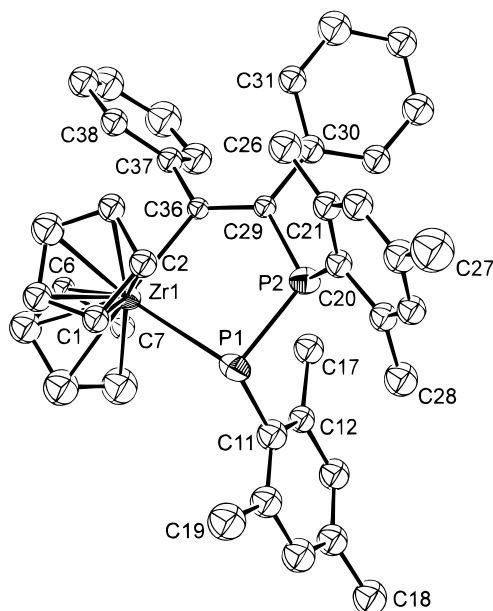
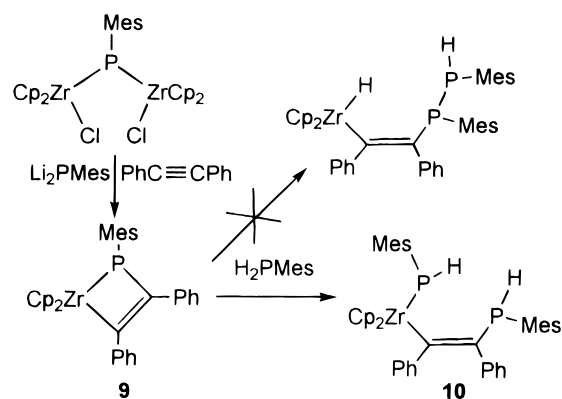


Figure 1. ORTEP drawing of **8**; 30% thermal ellipsoids are shown. Selected bond distances (Å) and angles (deg) are as follows: Zr(1)–P(1); 2.596(9); Zr(1)–C(36); 2.31(2); P(1)–P(2), 2.19(1); P(2)–C(29); 1.81(3); P(1)–Zr(1)–C(36); 89.0(7); Zr(1)–P(1)–P(2); 94.2(4); P(1)–P(2)–C(29); 111.8(9).

Scheme 1



conocene complex $\text{Cp}_2\text{Zr}(\text{N}_2\text{Ph}_2)(\text{THF})$ as described by Bergman and co-workers.²⁴

Insertion Reactions of 3. The reaction of *tert*-butyl isocyanide with **3** proceeded rapidly, giving a bright yellow product which was formulated as $\text{Cp}_2\text{Zr}(\text{C}(\text{N}-t\text{-Bu})\text{P}(\text{R}^*)\text{C}(\text{Ph})=\text{CPh})$ (**12**) on the basis of spectroscopic data (Scheme 2). Insertion into the Zr–P bond was consistent with the two low-field resonances in the ¹³C{¹H} NMR spectrum at 223.3 and 198.5 ppm. Preferential insertion into the Zr–P bond contrasts with reactions of related aza-²⁵ and oxametallacyclobutenes,²⁶ in which insertions occur exclusively at the Zr–C bond, but is compatible with the highly reactive nature of the Zr–P bond. The hapticity of the imino fragment was determined by an X-ray crystallographic study, which clearly showed η^2 coordination of the iminoacyl group

(24) Walsh, P. J.; Hollander, F. J.; Bergman, R. G. *J. Organomet. Chem.* **1992**, 428, 13.

(25) Hanna, T. A.; Baranger, A. M.; Walsh, P. J.; Bergman, R. G. *J. Am. Chem. Soc.* **1995**, 117, 3292.

(26) Vaughan, G. A.; Hillhouse, G. L.; Rheingold, A. L. *J. Am. Chem. Soc.* **1990**, 112, 7994.

(22) Bohra, R.; Hitchcock, P. B.; Lappert, M. F.; Leung, W.-P. *J. Chem. Soc., Chem. Commun.* **1989**, 728.

(23) Kurz, S.; Hey-Hawkins, E. *J. Organomet. Chem.* **1993**, 462, 203.

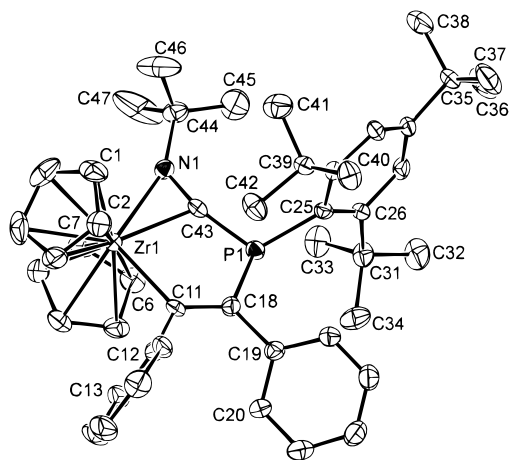


Figure 2. ORTEP drawing of **12**; 30% thermal ellipsoids are shown. Selected bond distances (Å) and angles (deg) are as follows: Zr(1)–N(1); 2.221(6); Zr(1)–C(43); 2.217(7); Zr(1)–C(11); 2.389(8); P(1)–C(18); 1.856(8); P(1)–C(43); 1.707(8); N(1)–C(43); 1.274(9); C(11)–Zr(1)–C(43); 73.0(3); C(11)–Zr(1)–N(1); 106.0(2); N(1)–Zr(1)–C(43); 33.3(2); C(43)–P(1)–C(18); 98.3(4).

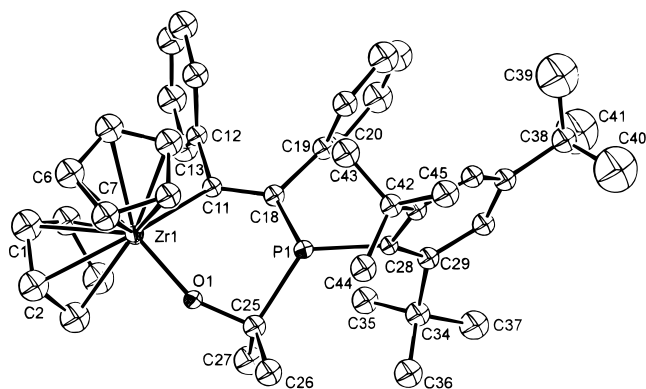
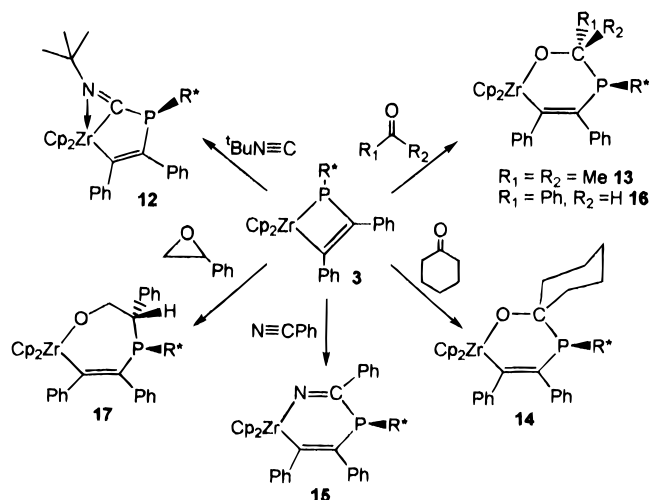


Figure 3. ORTEP drawing of **13**; 30% thermal ellipsoids are shown. Selected bond distances (Å) and angles (deg) are as follows: Zr(1)–O(1), 1.934(9); Zr(1)–C(11), 2.30(1); P(1)–C(18); 1.89(1); P(1)–C(25); 1.97(1); P(1)–C(28); 1.88(1); O(1)–Zr(1)–C(11); 87.1(5).

Scheme 2



to the zirconium center (Figure 2). The Zr(1)–C(43), Zr(1)–N(1), and C(43)–N(1) bond distances are very similar to those of the acyclic iminoacyl species $\text{Cp}_2\text{Zr}(\eta^2\text{-C}(\text{=NMe})\text{CHPh}_2)(\text{Me})$;²⁷ however, the cyclic nature of **12** enforces the “N-outside” coordination mode of the imino group. This coordination mode is disfavored in open-chain metallocene acyl and iminoacyl complexes²⁸ but has been previously observed in cyclic titanocene iminoacyls.²⁹ The pyramidal geometry about phosphorus in **12** and the resulting inequivalence of the cyclopentadienyl rings were not reflected in the temperature-invariant ¹H and ¹³C{¹H} NMR spectra.

Ketone and nitrile insertions also occurred into the Zr–P bond of **3**. For example, insertion of acetone rapidly produced the phosphaoxametallacyclohexene $\text{Cp}_2\text{Zr}(\text{OCMe}_2\text{P}(\text{R}^*))\text{C}(\text{Ph})=\text{C}(\text{Ph})$ (**13**) in 51% yield. Likewise, reactions of **3** with cyclohexanone and benzonitrile

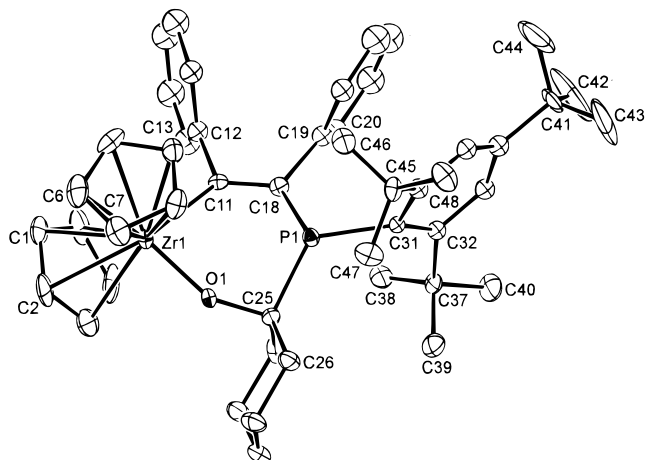


Figure 4. ORTEP drawing of **14**; 30% thermal ellipsoids are shown. Selected bond distances (Å) and angles (deg) are as follows. Molecule a: Zr(1)–O(1); 1.919(5); Zr(1)–C(11); 2.336(7); P(1)–C(18); 1.850(8); P(1)–C(25); 1.957(8); O(1)–Zr(1)–C(11); 85.8(2); Zr(1)–O(1)–C(25); 150.1(5).

afforded the similar six-membered metallacycles $\text{Cp}_2\text{Zr}(\text{O}(\text{c-CC}_5\text{H}_{10})\text{P}(\text{R}^*))\text{C}(\text{Ph})=\text{C}(\text{Ph})$ (**14**) and $\text{Cp}_2\text{Zr}(\text{N}=\text{C}(\text{Ph})\text{P}(\text{R}^*))\text{C}(\text{Ph})=\text{C}(\text{Ph})$ (**15**) in 58% and 46% yield, respectively (Scheme 2). X-ray crystallographic studies of **13** and **14** confirmed the formulations of the phosphaoxametallacyclohexenes (Figures 3 and 4, respectively). In each, the geometry at phosphorus is pyramidal and the $\text{C}_6\text{H}_2\text{-2,4,6-tert-Bu}_3$ substituent adopts an equatorial position relative to the ring. Unlike isocyanide insertion product **12**, the inequivalence of the cyclopentadienyl rings and methyl groups of **13** indicated by the solid-state structure was consistent with the ¹H NMR spectrum at –80 °C. The fluxionality of **13** was indicated by the single broad resonances observed in the room-temperature ¹H and ¹³C{¹H} NMR spectra ($\Delta G_c^\ddagger = 13.4$ kcal/mol). Variable-temperature NMR studies of **14** and **15** showed that they exhibited similar dynamic behavior corresponding to $\Delta G_c^\ddagger = 14.1$ and 13.0 kcal/mol, respectively. Related insertion of isonitrile into Zr–P and Hf–As bonds has recently been reported by Lindenberg *et al.*³⁰

A process involving a [4 + 2] retrocycloaddition of metallacycles **13–15** was indicated by reactivity studies. Addition of 1 equiv of benzaldehyde to **13** resulted in

(27) Cardin, D. J.; Lappert, M. F.; Raston, C. L. *Chemistry of Organo-Zirconium and -Hafnium Compounds*; Wiley: New York, 1986; pp 221–223.

(28) Tatsumi, K.; Nakamura, A.; Hofmann, P.; Stauffert, P.; Hoffmann, R. *J. Am. Chem. Soc.* **1985**, *107*, 4440.

(29) Campora, J.; Buchwald, S. L. *Organometallics* **1995**, *14*, 2039.

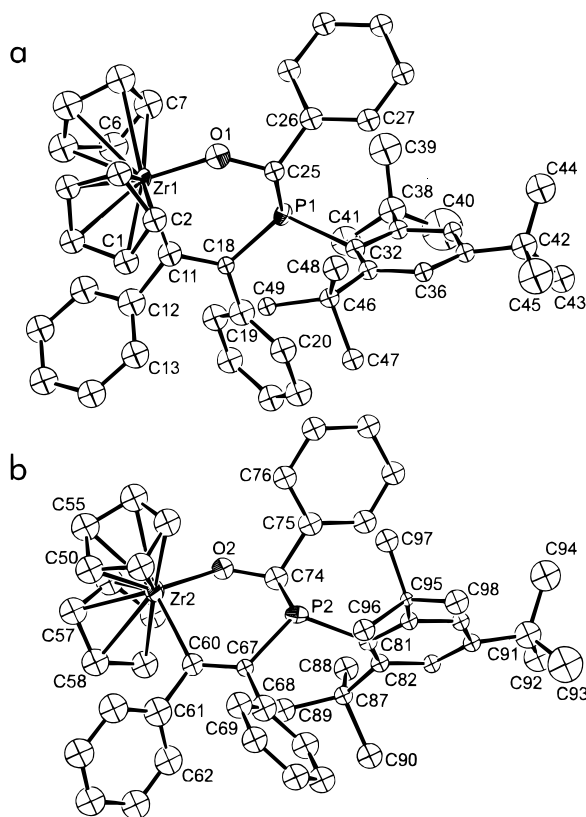


Figure 5. ORTEP drawing of the two molecules of **16** in the asymmetric unit; 30% thermal ellipsoids are shown. Selected bond distances (Å) and angles (deg) are as follows. Molecule a: Zr(1)–O(1); 1.97(3); P(1)–C(18); 1.83(3); P(1)–C(25); 1.94(4); P(1)–C(32); 1.94(2); O(1)–Zr(1)–C(11); 90(1). Molecule b: Zr(2)–O(2); 1.93(2); P(2)–C(67); 1.86(4); P(2)–C(74); 1.87(4); P(2)–C(81); 1.95(2); O(2)–Zr(2)–C(60); 86(1).

the liberation of free acetone and the formation of the metallacycle $\text{Cp}_2\text{Zr}(\text{OCHPhP}(\text{R}^*)\text{C}(\text{Ph})=\text{CPh})$ (**16**). Complex **16** was also formed through corresponding reactions with either **14** or **15**; as an alternative, **16** could be synthesized directly through the reaction of benzaldehyde with **3** to afford **16** in 61% yield (Scheme 2). The single resonance in the ^{31}P NMR spectrum of **16** attested to the diastereoselectivity of the insertion reaction. A subsequent X-ray crystallographic study revealed that the supermesityl group on phosphorus and the ketonic phenyl group both adopt equatorial positions and thus are *trans* with respect to the metallacyclic ring (Figure 5). In a similar way, reactions of **3** or **13**–**15** with 1 equiv of styrene oxide resulted in the formation of phosphaoxametallacycloheptene $\text{Cp}_2\text{Zr}(\text{OCH}_2\text{CHPhP}(\text{R}^*)\text{C}(\text{Ph})=\text{CPh})$ (**17**) in 68% yield (from **3**) (Scheme 2). X-ray crystallography was again employed to verify the selective formation of the *RR/SS* enantiomeric pair (Figure 6). In contrast to **13**–**15**, neither **16** nor **17** is a fluxional species; the solution ^1H and $^{13}\text{C}\{^1\text{H}\}$ NMR spectra are temperature invariant and correspond to the solid-state structures.

Kinetic studies of the reactions of **13** with either benzaldehyde or styrene oxide indicated a rate-limiting

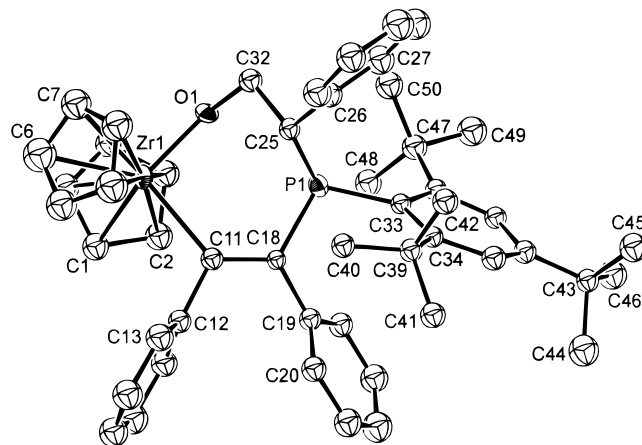
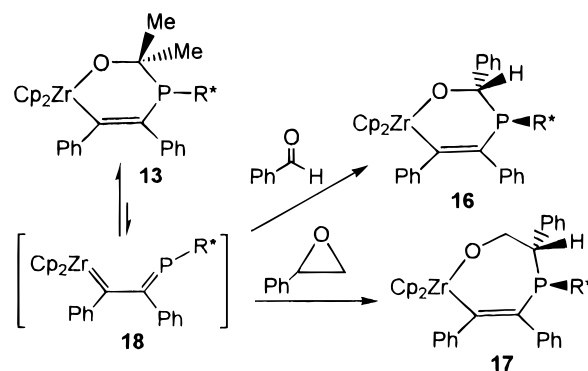


Figure 6. ORTEP drawing of **17**; 30% thermal ellipsoids are shown. Selected bond distances (Å) and angles (deg) are as follows: Zr(1)–O(1); 1.92(1); Zr(1)–C(11); 2.36(1); P(1)–C(18); 1.85(1); P(1)–C(25); 1.91(1); P(1)–C(33); 1.86(1); O(1)–Zr(1)–C(11); 96.2(4).

Scheme 3



loss of acetone from **13**, as the rate of reaction was independent of either benzaldehyde or styrene oxide concentration. We have previously communicated¹² that acetone is lost through a [4 + 2] retrocycloaddition, which generates zirconocene alkylidene intermediate **18**. A subsequent irreversible [4 + 2] cycloaddition with benzaldehyde yields **16**, while the ring opening of styrene oxide gives **17** (Scheme 3). Attempts to trap the zirconocene alkylidene intermediate with excess PMe_3 , pyridine, or 1-phenylpropyne were unsuccessful. However, the vinylimido complexes of titanocene described by Doxsee *et al.*³¹ and our report of the imido-phosphaalkene complex $(\text{Cp}_2\text{Zr}=\text{NC}(\text{Ph})=\text{PMe}_3^*)-(\text{PMe}_3)^{10c}$ are strong circumstantial evidence supporting the viability of intermediate **18**. In addition, similar [4 + 2] retrocycloadditions have been reported for azaoxametallacyclohexenes²⁵ and oxatitanacyclohexenes.³² Since ketone preferentially inserts into the metal–vinyl bond in these complexes, the [4 + 2] retrocycloadditions furnish $(\text{Cp}_2\text{M}=\text{O})_n$ along with either α,β -unsaturated imines or conjugated dienes.

A probable cause of the [4 + 2] retrocycloaddition in **13** is significant steric congestion in the six-membered ring. The observation of close contacts between both methyl groups and supermesityl *tert*-butyl fragments

(30) (a) Lindenberg, F.; Sieler, J.; Hey-Hawkins, E. *Polyhedron* **1996**, *15*, 459. (b) Lindenberg, F.; Müller, U.; Pilz, A.; Sieler, J.; Hey-Hawkins, E. *Z. Anorg. Allg. Chem.* **1996**, *622*, 683.

(31) (a) Doxsee, K. M.; Farahi, J. B. *J. Chem. Soc., Chem. Commun.* **1990**, 1452. (b) Doxsee, K. M.; Farahi, J. B.; Hope, H. *J. Am. Chem. Soc.* **1991**, *113*, 8889.

(32) Doxsee, K. M.; Mouser, J. K. M. *Tetrahedron Lett.* **1991**, *32*, 1687.

(five H...H distances ranging from 2.098 to 2.234 Å) in the solid-state structure support this premise. Substitution of a methyl group with a hydrogen atom (e.g. in **16**) results in a stable complex in which [4 + 2] retrocycloadditions are not provoked.

Sterically Induced Epimerization at Phosphorus. A feature common to metallacyclobutenes **3**, **5**, **6**, and **9**, metallacyclopentenes **8** and **12**, and metallacyclohexenes **13**–**15** is the discrepancy between the spectroscopic data and the expected pyramidal geometry at phosphorus. This geometry imposes inequivalent environments on the two cyclopentadienyl rings; however, each of these complexes exhibit only one resonance, or two very broad resonances in the case of **14**, attributable to these ligands in the room-temperature ^1H and $^{13}\text{C}\{-^1\text{H}\}$ NMR spectra. This indicates either a planar geometry or rapid inversion at phosphorus. These alternatives could not be distinguished for **3** or **5**, as cooling to -80°C merely resulted in the observation of line broadening. In comparison, a pyramidal configuration has been confirmed crystallographically for **8** and **12**–**14**.

The kinetic studies described for **13** revealed a rate-limiting loss of acetone, thus indicating the lack of a rapid equilibrium between **13** and zirconocene alkylidene intermediate **18**. Furthermore, variable-temperature NMR studies of **13**–**15** yielded values of ΔG_c^\ddagger consistent with a reduced barrier to inversion at phosphorus. In a similar way, preliminary kinetic investigations of the [2 + 2] retrocycloadditions exhibited by phosphametallacyclobutenes **3** and **5** revealed a rate-limiting loss of alkyne. These data, as well as ^1H and $^{13}\text{C}\{^1\text{H}\}$ NMR data, indicate that the cause of the fluxional process for these metallacycles is rapid inversion at phosphorus rather than ring fragmentation.

Similar to the four- and six-membered metallacycles, the NMR spectra of metallacyclopentenes **8** and **12** were also inconsistent with metallacycle fragmentation. Furthermore, neither complex underwent dissociative exchange with alkyne or PMe_3 . The NMR spectra of **12** were temperature-invariant; however, NMR spectra of **8** showed a marked temperature dependence. The broad resonance due to the cyclopentadienyl rings split and sharpened into two lines upon cooling to -80°C ($\Delta G_c^\ddagger = 13.8 \text{ kcal mol}^{-1}$). The activation barrier is within the range expected for metal-assisted inversion at phosphorus, and the averaging of the cyclopentadienyl resonances further implies that the process is occurring at *both* phosphorus centers.

The feature common to the family of four-, five-, and six-membered phosphametallacycles is considerable steric congestion. We have previously suggested that delocalization of the phosphorus lone pair into the p orbital of the alkenyl moiety stabilizes a planar geometry at phosphorus and consequently lowers the inversion barrier.¹² This view is incompatible with subsequent molecular orbital calculations, which indicate no such extended π -interaction. The imposition of a planar geometry at phosphorus also places the lone pair in an orbital which is orthogonal to the vacant $1a_1$ orbital of the zirconocene fragment. Furthermore, total energy EHMO calculations for the model $\text{Cp}_2\text{ZrPH}(\text{HCCH})$ indicate that a pyramidal geometry at phosphorus is about 60 kJ/mol more favorable than a planar configuration (Figure 7). The LUMO is the $1a_1$ orbital of the Cp_2M fragment,³³ while the HOMO is largely the

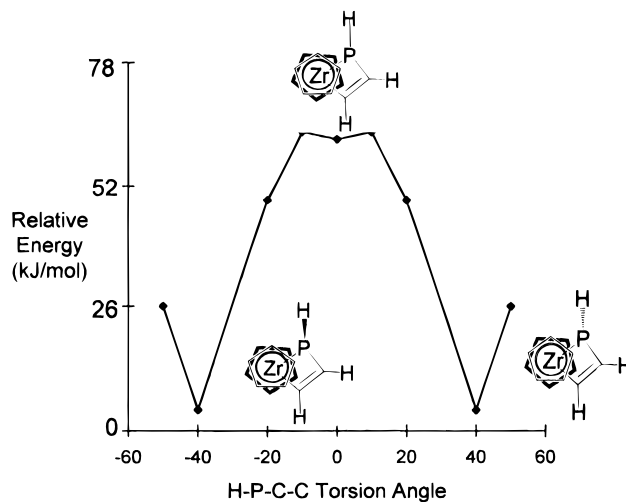


Figure 7. Plot of the EHMO total energy of the model $\text{Cp}_2\text{ZrPH}(\text{HCCH})$ as a function of the H–P–C–C torsion angle.

phosphorus p orbital in which the phosphorus lone pair resides. Regardless of the geometry at phosphorus, no evidence was indicated either for an extended π -system involving the lone pair on phosphorus and the alkenyl π -bond or M–P multiple bonding.

From the kinetic and computational studies presented in this paper, it is clear that steric effects in our family of metallacycles are manifested in two ways: reduced inversion barriers at phosphorus and the [4 + 2] retrocycloadditions of **13**–**15**. Interestingly, phosphaoxametallacyclohexene **16** and phosphaoxametallacycloheptene **17** are immune to both effects. This may be attributed to reduced steric constraints due to the presence of a hydrogen substituent on the metallacyclic carbon atom α to phosphorus. Increased steric demands (as in **13**–**15**) result in the observed destabilization of the metallacycle and dynamic behavior.

Summary

In summary, the first examples of phosphametallacyclobutenes exhibit intriguing chemistry, such as [2 + 2] retrocycloadditions and insertions of unsaturated polar organic molecules into the Zr–P bond. These and related reactions have provided access to a family of four-, five-, and six-membered phosphametallacycles. Steric factors exert considerable influence over the entire group of complexes and are manifested as reduced inversion barriers at phosphorus and [4 + 2] retrocycloadditions. In contrast, the phosphametallacyclohexene derived from aldehyde insertion is not fluxional. Furthermore, the insertion proceeds with a high degree of P/C diastereoselectivity, a feature which augurs well for future applications of these metallacycles in enantioselective syntheses.

Acknowledgment. Support from the NSERC of Canada is acknowledged. T.L.B. is grateful for the award of an NSERC postgraduate scholarship.

Supporting Information Available: Tables of atomic coordinates, thermal parameters, and bond distances and angles for **8**, **12**–**14**, **16**, and **17** (53 pages). Ordering information is given on any current masthead page.

OM9607053